Impact of Selenium and Vitamin E Deficiency on Zika Virus Pathogenesis and Immune Response in Mice

Olukunle O Oluwasemowo , Monica Elaine Graham , James B Thissen , Aram Avila-Herrera , Jeffrey A Kimbrel , Deepa K Murugesh , Dina R. Weilhammer , Tanya Tanner , Nicole M Collette , Monica K Borucki *

Posted Date: 16 December 2025

doi: 10.20944/preprints202512.1390.v1

Keywords: Zika virus; selenium; vitamin E; mutation; nutrition; cytokine; neuroinvasion; quasispecies

 doi:10.20944/preprints202512.1390.v1

Article

Impact of Selenium and Vitamin E Deficiency on Zika Virus Pathogenesis and Immune Response in Mice

Olukunle O. Oluwasemowo [1], Monica E. Graham [1], James B. Thissen [1], Aram Avila-Herrera [2], Jeffrey A. Kimbrel [2], Deepa K. Murugesh [1], Dina R. Weilhammer [1], Tanya Tanner [1], Nicole M. Collette [1] and Monica K. Borucki [1,*]

[1] Lawrence Livermore National Laboratory, Physical and Life Sciences Directorate, Biotechnology and Biosciences Division, Livermore, CA, United States of America.

[2] Lawrence Livermore National Laboratory, Computing Directorate, Global Security Computing Division, Livermore, CA, United States of America.

* Correspondence: borucki2@llnl.gov

Abstract

Micronutrient status is recognized to influence host susceptibility to viral infections, yet its impact on Zika virus (ZIKV) pathogenesis remains incompletely understood. We investigated the effects of dietary selenium and combined selenium plus vitamin E deficiency on ZIKV infection outcomes in a murine model. Mice maintained on deficient diets exhibited significantly lower neutralizing antibody titers and reduced levels of key antiviral cytokines (IFN-γ, TNF-α, IFN-α, IFN-β, IL-12p70, CCL5) compared to controls. Correspondingly, higher viral RNA loads were detected in the brains of double-deficient mice, which also experienced greater weight loss and increased mortality. Deep sequencing revealed no major differences in overall viral genome diversity across diet groups; however, specific mutations, including V330L and D67E in the E gene, and V360I in the NS3 gene, were enriched or detected in nutritionally deficient animals. These findings suggest that antioxidant micronutrient deficiency impairs both humoral and cellular immune responses to ZIKV potentially facilitating enhanced neuroinvasion. While the functional consequences of the identified mutations warrant further investigation, our results underscore the importance of adequate micronutrient intake for optimal antiviral defense. Further studies are needed to clarify the epidemiological significance of these observations.

Keywords: Zika virus; selenium; vitamin E; mutation; nutrition; cytokine; neuroinvasion; quasispecies

1. Introduction

Selenium and vitamin E are essential micronutrients that function synergistically as critical components of the host antioxidant defense system [1–4]. The impact of selenium and/or vitamin E deficiency on viral pathogenesis has been extensively documented through both experimental and clinical studies, thereby demonstrating that nutritional deficiencies can fundamentally alter host-pathogen interactions and disease outcomes [5–12]. Geographic regions characterized by selenium-depleted soils have consistently reported more severe manifestations of infectious diseases, including viral infections [13,14], as well as more pronounced noninfectious disease outcomes [15,16]. In contrast, targeted supplementation with selenium and/or vitamin E has shown therapeutic benefits by improving disease progression and clinical outcomes [17–19].

Selenium is an essential cofactor for more than 25 selenoproteins, which are involved in a wide range of biological processes, including redox signaling, antioxidant defense, thyroid hormone metabolism, and regulation of both innate and adaptive immune responses [20,21]. Among these,

 doi:10.20944/preprints202512.1390.v1

glutathione peroxidases, thioredoxin reductases, and selenoprotein P are particularly critical for maintaining cellular redox homeostasis and protecting tissues from oxidative stress [22]. Vitamin E, primarily in the form of α-tocopherol, acts as a potent lipid-soluble antioxidant, neutralizing reactive oxygen species and preserving membrane integrity [23]. The interdependent relationship between selenium and vitamin E is exemplified by their ability to compensate for each other's antioxidant activities, with selenium-dependent glutathione peroxidases (GPx) protecting against lipid peroxidation when vitamin E levels are inadequate [24,25] and vitamin E partially compensating for the loss of selenium-dependent GPx4 [1,26].

Emerging evidence suggests that climate change is exacerbating global selenium deficiency by altering precipitation patterns and soil chemistry, thereby reducing selenium bioavailability in many regions [27,28]. This environmental shift has far-reaching consequences for human and animal health, as selenium deficiency not only impairs antiviral immune responses but also accelerates the emergence of more virulent viral variants by increasing viral mutation rates and immune selection pressure [29]. This phenomenon is particularly pronounced in RNA viruses, which inherently possess high mutation rates due to the error-prone nature of their RNA-dependent RNA polymerases, leading to the rapid generation of genetically diverse viral populations or quasispecies [30,31]. Under conditions of oxidative stress associated with micronutrient deficiencies, RNA virus mutation rates can increase dramatically, creating evolutionary bottlenecks that select for variants with enhanced virulence, immune evasion capabilities, or altered tissue tropism [32]. These findings underscore a critical intersection between environmental change, nutritional status, and infectious disease dynamics. Predictive modeling indicates that climate-driven selenium deficiency may continue to expand globally, potentially affecting billions and creating ecological conditions favorable for viral evolution thereby increasing the risk of future pandemics [27,33].

Zika virus (ZIKV), a mosquito-borne flavivirus closely related to yellow fever virus, West Nile virus, and dengue virus, has emerged as a significant global health threat, especially following the devastating 2015-2016 pandemic that affected over 70 countries and territories [34,35]. As a positive-sense single-stranded RNA virus, ZIKV inherently exhibits a high mutation rate due to the lack of proofreading activity in its RNA-dependent RNA polymerase, resulting in the formation of genetically diverse viral quasispecies within infected hosts [36,37]. This genetic plasticity enables rapid adaptation to selective pressures, including those imposed by host immunity and antiviral treatments [38,39].

Clinically, ZIKV infection is associated with severe neurological complications, including microcephaly in developing fetuses, Guillain-Barré syndrome in adults, and other neurotropic manifestations [40,41]. The virus's capacity for rapid geographic spread, neurotropism, persistence in immune-privileged sites, and propensity for genetic evolution has led the World Health Organization to designate ZIKV as a priority pathogen with significant re-emergence and pandemic potential [42,43]. Importantly, the evolutionary dynamics of RNA viruses like ZIKV are highly sensitive to host nutritional status, as oxidative stress associated with micronutrient deficiencies can further increase mutation rates and facilitate the selection of variants with enhanced virulence or immune escape [29,44].

Despite extensive research on ZIKV pathogenesis, the molecular mechanisms by which micronutrient deficiencies influence viral evolution, tissue tropism, and host immune responses remain poorly understood. The combination of intrinsic genetic instability in RNA viruses and the oxidative stress environment created by selenium and vitamin E deficiency may accelerate viral mutation rates and promote the emergence of variants with altered tissue tropism, enhanced virulence, or increased pandemic potential [32,36]. Given the established role of these micronutrients in antiviral immunity and the global trend toward increasing deficiency states, investigating their impact on ZIKV evolution and pathogenesis addresses a critical knowledge gap with significant implications for pandemic preparedness and therapeutic intervention strategies.

This study aimed to elucidate the genotypic, immunological, and phenotypic changes associated with ZIKV infection in hosts experiencing combined selenium and vitamin E deficiency, with

 doi:10.20944/preprints202512.1390.v1

particular emphasis on understanding how nutritional status influences viral tissue distribution, disease severity, and the potential emergence of viral variants with enhanced pathogenic properties and pandemic potential.

2. Materials and Methods

2.1. Virus Stocks

Two Asian strains of ZIKV were utilized for murine infection in this study: the epidemic strain PRVABC59 (isolated in Puerto Rico, 2015) and the pre-epidemic strain FSS13025 (isolated in Cambodia, 2010). The PRVABC59 strain (Human/2015/Puerto Rico) was obtained from BEI Resources (NR-50240) while the FSS13025 strain was obtained from the University of Texas Medical Branch (UTMB) Arbovirus Reference Collection. Viral stocks were prepared by one or two passages in Vero cells. Infectious titers were determined using plaque assay method, as previously described [45].

2.2. Mouse Diets

Three distinct dietary regimens were used for the experimental mice: a nutritionally adequate, normal diet (ND), a selenium-deficient diet (SD), and a selenium plus vitamin E double-deficient diet (SED). All diets were specially formulated and commercially supplied by TEKLAD (TD.92163). The expected selenium content of these diets is based on previously published analyses of similar formulations from the same vendor [46], which demonstrated that the Se-adequate diet aligns with selenium levels considered sufficient in humans, while the Se-deficient and SED diets correspond to levels associated with deficiency [47]. Although direct measurement of selenium concentrations in our dietary batches was not performed, we confirmed the functional adequacy of the ND by assessing higher GPx activity [48] in the sera of mice fed this diet compared to the SD and SED groups. Detailed compositions of each diet are provided in the Supplemental Information (Supplementary Table S1).

2.3. In Vivo Infections

ZIKV does not suppress type I interferon (Ifnar1) expression in mice as it does in humans, rendering wild-type mice resistant to disease. To overcome this limitation, we utilized a mouse strain lacking the type I interferon α/β receptor (Ifnar1−/−), which is susceptible to ZIKV infection and widely used for studies of ZIKV pathogenesis [49,50].

Type I interferon α/β receptor knockout (Ifnar1−/−) mice, approximately three weeks old, were obtained from Jackson Laboratories (Bar Harbor, ME, USA) and housed in the Animal Care Facility at Lawrence Livermore National Laboratory (LLNL) under protocols approved by the LLNL Institutional Animal Care and Use Committee (approval number 22-10-058 (315)).

Mice were randomly assigned to three dietary cohorts. The control group received a nutritionally complete (normal) diet (ND), while experimental groups were fed either a selenium-deficient diet (SD) or a selenium and vitamin E double-deficient diet (SED). Diets were administered for 5 to 6 weeks prior to infection to ensure depletion of respective micronutrient stores, as previously described [51] with the control group maintained on the normal diet for the same duration.

Micronutrient status was assessed by measuring glutathione peroxidase (GPx) activity and alpha-tocopherol (TCPa) concentrations in mouse serum, serving as proxies for selenium and vitamin E levels, respectively. GPx activity was determined using the Glutathione Peroxidase Assay Kit (MAK437-1KT; Sigma-Aldrich) according to the manufacturer's instructions and serum TCPa concentrations were quantified using the General Alpha-Tocopherol (TCPa) ELISA Kit (MBS2000369; MyBiosource) following the manufacturer's protocol.

For infection, virus stocks containing approximately 3.8×10^6 PFU/mL were used, with sterile phosphate-buffered saline (PBS) serving as the mock infection control. Mice were lightly anesthetized with isoflurane prior to subcutaneous administration of 0.05 mL of the virus stock into the right hind limb. Baseline body weights were recorded at the time of infection, and subsequent weights were

 doi:10.20944/preprints202512.1390.v1

measured daily until the termination of the experiment. All animals were observed at least once daily for clinical signs of illness, including lethargy, ruffled fur, hunched posture, and neurological symptoms such as paralysis and tremors. Mortality was documented, and any mouse exhibiting a weight loss exceeding 20% of its baseline value was humanely euthanized prior to the scheduled experimental endpoint.

2.4. Sample Collection

Sample collection was performed at two predetermined timepoints, corresponding to peak viremia [6 days post-infection, (dpi)] and tissue pathology (14 dpi). At each experimental endpoint, mice were humanely euthanized using controlled atmosphere CO_2 stunning in accordance with institutional guidelines. At 6 dpi, whole blood samples were collected via cardiac puncture for nucleic acid extraction, viral genome quantification, deep sequencing analysis and immunological cytokine profiling. At 14 dpi, blood samples were collected for neutralizing antibody quantification. In addition, brain and reproductive tissues (ovaries in females, testes in males) were harvested at 14 dpi for further analysis.

For molecular evaluation, tissue samples were preserved in RNAlater solution (Invitrogen, Carlsbad, CA, USA) for subsequent nucleic acid extraction, viral genome quantification, and deep sequencing. All sample collection procedures were performed under aseptic conditions. Samples designated for molecular analysis were either processed immediately or stored at -80°C and processed at the earliest possible time to maintain sample integrity and minimize RNA degradation.

2.5. Sample Processing and RNA Extraction

Whole blood samples were allowed to clot at room temperature for 30 minutes and subsequently centrifuged at 1,500 × g for 10 minutes at 4°C to separate serum. The serum fraction was carefully collected and stored at -80°C until nucleic acid extraction.

Tissues preserved in RNAlater were removed and excess solution was blotted away. Approximately 30 mg of reproductive tissue (testes or ovaries) and 50 mg of brain tissue were weighed and transferred into sterile tubes containing 3 mm ceramic beads. Each sample was lysed in 600 µL of RLT buffer (Qiagen, Hilden, Germany) supplemented with β-mercaptoethanol, then homogenized using an Omni Bead Ruptor homogenizer according to the manufacturer's protocol.

Total RNA was extracted from homogenized tissues using the RNeasy Mini Kit (Qiagen, Hilden, Germany) with on-column DNase I treatment (Qiagen) to remove genomic DNA. RNA was eluted in 65 µL of RNase-free water and stored at -80°C until further analysis. For serum samples, RNA was extracted from 140 µL of serum using the RNeasy Mini Kit (Qiagen) according to the manufacturer's instructions. RNA was eluted in 65 µL of RNase-free water and stored at -80°C.

2.6. Quantification of Viral RNA Genome

ZIKV genome copy numbers were determined using one-step quantitative reverse transcription PCR (RT-qPCR). Reactions were performed with PrimeTime One-Step RT-qPCR Master Mix (Integrated DNA Technologies) using ZIKV-specific primers and probe: forward primer ZIKV_835, reverse primer ZIKV_911c, and probe ZIKV_860 [52]. Absolute quantification was achieved by generating a standard curve from a synthetic RNA standard of known concentration (Genscript, Piscataway, NJ, USA).

RT-qPCR was performed under the following thermal cycling conditions: initial reverse transcription at 98°C for 30 seconds, followed by 40 cycles of denaturation at 98°C for 15 seconds, annealing at 64°C for 20 seconds, and extension at 72°C for 1.2 minutes, with a final extension at 72°C for 10 minutes. All samples were analyzed in duplicate. Viral genome copies per microliter of serum or milligram of tissue were calculated after correcting for serum volume or tissue weight respectively.

 doi:10.20944/preprints202512.1390.v1

2.7. Immunological Cytokines Profiling

To evaluate the effect of dietary selenium and vitamin E deficiency on the immune response to ZIKV infection, serum cytokine levels were analyzed in mice maintained on the three diets: ND, SD, and SED. Blood samples were collected at 6 dpi from ZIKV-infected mice, while blood from mock-infected (PBS-injected) mice in each dietary group served as controls.

Serum cytokine concentrations were determined using the LEGENDplex™ Mouse Anti-Virus Response Panel 13-plex assay (BioLegend, San Diego, CA, USA), following the manufacturer's protocol. Briefly, serum samples collected at 6 dpi were thawed on ice and diluted two-fold with Matrix A reagent provided in the kit. Flow cytometric analysis was performed using a BD FACSCelesta™ Cell Analyzer (BD Biosciences, Franklin Lakes, NJ, USA). Instrument settings and compensation were established using the kit's setup and control beads in accordance with the LEGENDplex™ protocol. For each sample, a minimum of 300 events per analyte region was acquired to ensure statistical reliability.

Raw flow cytometry data were processed using the LEGENDplex™ Data Analysis Software Suite (https://www.biolegend.com/en-ie/immunoassays/legendplex/support/software), which enabled automated gating, standard curve generation, and quantification of cytokine concentrations. The 13-plex panel measured the following cytokines: IFN-α, IFN-β, IFN-γ, IL-6, TNF-α, IL-1β, IL-10, IL-12p70, IP-10 (CXCL10), MCP-1 (CCL2), IL-17A, IFN-λ2/3, and IFN-λ1. Cytokine levels from ZIKV-infected mice were normalized to those from PBS-injected controls within each diet group.

2.8. Plaque Reduction Neutralization Test (PRNT)

The PRNT assay was performed as previously described [53], with modifications as detailed below. Vero/TMPRSS2 cells [45] were cultured in 24-well plates for the assay. Serum samples collected from mice 14 days post ZIKV infection was used. Six samples were randomly selected from each dietary group: ND, SD, and SED. Blood samples were allowed to clot, and serum was separated by centrifugation. Vero/TMPRSS2 cells were seeded in 24-well plates and grown to 80–90% confluency. Serum samples were heat-inactivated at 56°C for 30 minutes. Serial three-fold dilutions of each serum sample were prepared in DMEM. Equal volumes of diluted serum and ZIKV (at a predetermined concentration to achieve 30–50 plaques per well in the virus control) were mixed and incubated at 37°C for 1 hour to allow neutralization. After incubation, 200 µL of the virus-serum mixture was added to each well and incubated at 37°C for 1 hour with gentle rocking every 15 minutes. The inoculum was then removed, and cells were overlaid with DMEM containing 1% methylcellulose and 2% FBS. Plates were incubated at 37°C in 5% CO_2 for 4–5 days. Following incubation, cells were stained with 1% crystal violet to visualize plaques. Plaques were counted, and the percentage of plaque reduction was calculated relative to virus-only controls. The $PRNT_{50}$ titer was defined as the highest serum dilution resulting in a 50% reduction in plaque number compared to the virus control. All samples were assayed in duplicate, and appropriate negative and positive controls were included in each run.

2.9. Amplicon-Based ZIKV Sequencing

2.9.1. Primer Design

A custom primer set (designated M1000 primers) was designed for multiplex amplification of ZIKV strains PRVABC59 and FSS13025 using the Primal Scheme web-based primer design tool (https://primalscheme.com/) [54]. The set included 12 primer pairs, each generating amplicons of approximately 1,000 nucleotides with overlaps of 114–157 nucleotides, ensuring complete coverage of the ~11 kb ZIKV genome. In a pilot study, the M1000 primers demonstrated improved genome coverage compared to previously published primer sets [55] as shown in Supplementary Figure S2. Primer sequences are provided in the supplementary materials (Supplementary Table S2).

 doi:10.20944/preprints202512.1390.v1

2.9.2. RT-PCR

Whole-genome sequencing of ZIKV was performed using an amplicon-based approach with the M1000 primers, following a protocol similar to Grubaugh et al. [55]. First-strand cDNA synthesis was performed using 7 µL of extracted RNA and the LunaScript® RT SuperMix Kit (New England Biolabs) with the following conditions: 25°C for 10 minutes, 50°C for 10 minutes, 85°C for 5 minutes, then held at 4°C.

For PCR amplification, 2.5 µL of cDNA per reaction was used. The 12 primer pairs were divided into two pools (Pool 1 and Pool 2), each containing 6 primer pairs prepared from equal volumes of 10 µM primer stocks. Two multiplex PCR reactions were set up for each sample, one for each primer pool, using 2.5 µL of the respective primer pool. PCR was performed with Q5 High-Fidelity DNA Polymerase (New England Biolabs) under the following cycling conditions: initial denaturation at 98°C for 30 seconds, followed by 35 cycles of 95°C for 15 seconds and 65°C for 5 minutes, with a final hold at 4°C. Amplification success was confirmed by electrophoresis of 5 µL of PCR products on 1% agarose gels.

2.9.3. Library Preparation and Sequencing

Amplicons from the ZIKVprimer pools were combined in equal volumes to create a total of 20 µL pooled product per sample. Pooled amplicons were purified using 0.7× AMPure XP magnetic beads (Beckman Coulter) according to the manufacturer's standard protocol and eluted in 22 µL of nuclease-free water. Purified PCR products were quantified using a Qubit 4.0 fluorometer (Thermo Fisher Scientific).

Sequencing libraries were prepared using 50 ng of purified amplicons as input for the Illumina DNA Prep library preparation kit (Illumina), following the manufacturer's protocol for small amplicons. Completed libraries were quantified and quality-assessed using the TapeStation 4200 system (Agilent Technologies). Libraries were normalized to 4 nM, pooled in equimolar ratios, and diluted to a final loading concentration of 750 pM for sequencing on the Illumina NexSeq 2000 platform using a P1 300 cycle (2×150 bp) kit with onboard denaturation and dilution. Raw sequencing data have been deposited in the NCBI Sequence Read Archive under BioProject accession number PRJNA1374194.

2.10. Bioinformatics Analysis

Variant calling and sequence analysis were performed using Mappgene (https://github.com/LLNL/mappgene), a comprehensive variant calling pipeline designed for high-performance computing environments [56]. The Mappgene pipeline integrates multiple bioinformatics tools: BWA-MEM v0.7.17 for read alignment to the ZIKV reference genome (PRVABC59, GenBank: KU501215.1), iVar v1.4.3 for primer trimming, read filtering, and variant calling, and LoFreq v2.1.5 for additional variant detection.

Raw sequencing reads underwent quality control and preprocessing, with high-quality reads aligned to the reference genome using default BWA-MEM parameters. Post-alignment processing included automated primer sequence removal and consensus sequence generation requiring a minimum coverage depth of 10× and a minimum variant frequency of 75%. Variants were filtered based on quality scores (minimum Phred score of 20), coverage depth (minimum 100× for variant positions), and allele frequency thresholds (minimum 1% for minority variants, 75% for consensus-level variants).

2.11. Statistical Analysis

Statistical analyses were performed using GraphPad Prism version 10.0 (GraphPad Software, San Diego, CA, USA) and R version 4.5.0 [57]. Data are presented as mean ± standard deviation, unless otherwise indicated. Viral load comparisons across multiple groups were analyzed using two-way analysis of variance (ANOVA) followed by Tukey's multiple comparison test. Glutathione

 doi:10.20944/preprints202512.1390.v1

peroxidase (GPx) activity was assessed using the Kruskal-Walli's test. Longitudinal weight data were evaluated using a mixed-effects model with restricted maximum likelihood (REML) estimation. Neutralizing antibody titers (PRNT) were analyzed using ordinary one-way ANOVA with appropriate post hoc comparisons. Cytokine concentration values were $\log_{10}$ transformed then analyzed using ordinary one-way ANOVA with multiple comparisons and appropriate post hoc comparisons. Statistical significance was defined as $p < 0.05$. All tests were two-tailed.

3. Results

A total of 120 Ifnar1−/− mice were used in this study, with equal numbers allocated to two experimental endpoints: day 6 and day 14 (Table 1). For the day 6 endpoint, 60 serum samples were collected. For the day 14 endpoint, 180 samples were obtained, comprising serum, brain, and reproductive tissues from each mouse.

Table 1. Description of samples analyzed.

Duration of experiment	Diet Groups	Number of Mice	Samples Analyzed
Day 0 – Day 6	ND	20	Serum$^{*\#P}$
	SD	20	Serum$^{*\#P}$
	SED	20	Serum$^{*\#P}$
Day 0 – Day 14	ND	20	Serum^{s}, Brain$^{*\#}$, reproductive tissue$^{*\#}$
	SD	20	Serum^{s}, Brain$^{*\#}$, reproductive tissue$^{*\#}$
	SED	20	Serum^{s}, Brain$^{*\#}$, reproductive tissue$^{*\#}$
Total		**120**	

Analysis performed: * = qPCR, # = whole genome sequencing, π = cytokine profiling, σ = neutralizing antibody evaluation.

3.1. GPx Activity and Vitamin E Levels in Nutritionally Deficient Groups

Glutathione peroxidase (GPx) activity is highly dependent on selenium levels, since selenium is required for its catalytic function [4,58]. Therefore, measurement of GPx activity provides a sensitive and specific readout of selenium status in the experimental mouse cohorts. Serum GPx activity was significantly reduced in mice fed the selenium-deficient (SD) diet compared to the normal diet (ND) group ($p = 0.0145$; Figure 1-A). Mice maintained on the selenium and vitamin E-deficient (SED) diet showed similar trend of reduced GPx activity relative to the ND group. Serum alpha-tocopherol (TCPa) concentrations were assessed using a competitive ELISA, in which higher detected TCPa signals correspond to lower actual vitamin E concentrations in the sera. Accordingly, the SED group exhibited the highest TCPa signal, reflecting the lowest level of vitamin E among the groups ($p = 0.0493$; Figure 1-B).

 doi:10.20944/preprints202512.1390.v1

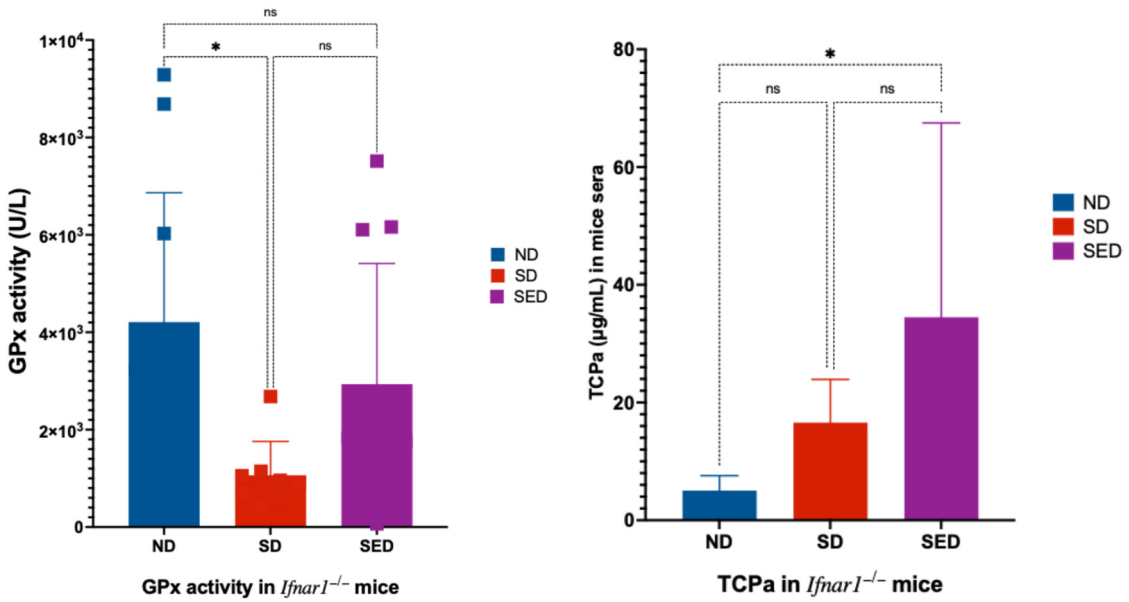

Figure 1. Serum selenium and vitamin E status in mice after dietary intervention. (A) Glutathione peroxidase (GPx) activity and (B) alpha-tocopherol (TCPa) concentration in the serum of mice after more than five weeks on normal diet (ND), selenium-deficient diet (SD), or selenium and vitamin E-deficient diet (SED). TCPa levels were measured by competitive ELISA, with higher assay signal indicating lower vitamin E concentration.

3.2. Severity of ZIKV Infection in Selenium and Vitamin E Double-Deficient Mice

Body weight loss is commonly used as a marker for disease severity in ZIKV-infected mice [59,60]. We hypothesized that selenium and vitamin E deficiency, will lead to a more severe ZIKV disease outcome, especially, since deficiencies in these micronutrients have been shown to exacerbate the severity of viral infections in animal models [8,61]. Body weight remained stable in all PBS-injected mice, regardless of diet (Figure 2-A). In contrast, Zika virus-infected mice exhibited significant weight loss ($p < 0.001$) beginning at 3 dpi, with the greatest decline at 9–10 dpi. Zika-infected mice on the normal diet (ND_ZIKV) and selenium-deficient diet (SD_ZIKV) experienced similar weight loss ($p = 0.1616$). However, Zika-infected mice on the selenium and vitamin E double-deficient diet (SED_ZIKV) lost the most weight, and three mice in this group died at 9 dpi. Weight loss patterns in the combined male and female data (Figure 2-A) were consistent when males (Figure 2-B) and females (Figure 2-C) were analyzed separately.

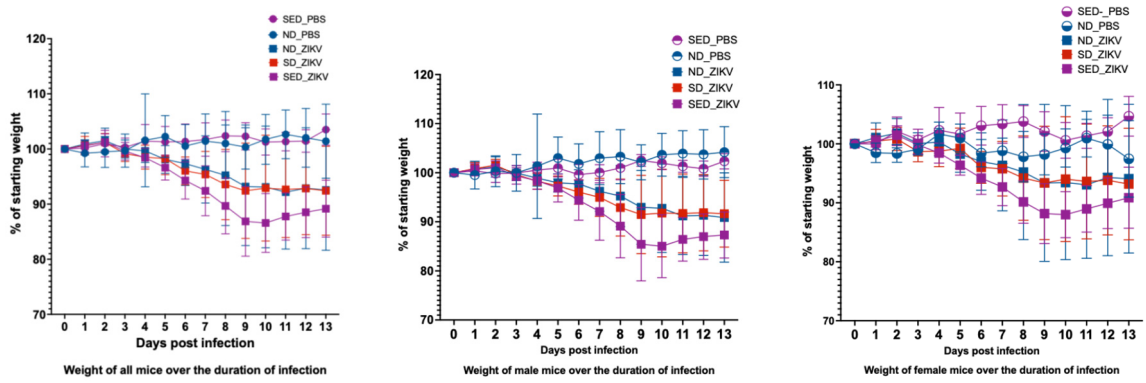

Figure 2. Percentage weight change in mice during ZIKV infection. Average daily weight is shown as percentage of starting weight for each group throughout the course of infection. (A) Combined male and female data. (B) Male only. (C) Female only. Groups are defined as follows: SED_PBS: PBS-injected mice on selenium and vitamin E double-deficient diet; ND_PBS: PBS-injected mice on normal diet; ND_ZIKV: Zika virus-infected mice on normal diet; SD_ZIKV: Zika virus-infected mice on selenium-deficient diet; SED_ZIKV: Zika virus-infected mice on selenium and vitamin E double-deficient diet.

 doi:10.20944/preprints202512.1390.v1

3.3. ZIKV RNA Levels in Brain Tissue of Selenium and Vitamin E Double-Deficient Mice

ZIKV viremia typically peaks within the first week after infection [59,60], and preliminary studies in our laboratory (data not shown) identified day 6 post-infection as the peak of viremia in our model. Preliminary experiments also demonstrated that the PRVABC59 strain yielded significantly higher viral genome copies in sera of mice compared to FSS13025 (Supplemental Figure S1). Consequently, subsequent experiments were conducted exclusively with the PRVABC59 strain. There is substantial evidence that ZIKV can persist in immune-privileged organs (including the brain and reproductive tissues) beyond the acute phase, contributing to neurological and reproductive pathologies [62–64]. We hypothesized that selenium and vitamin E deficiency could aggravate ZIKV systemic replication and persistence. Therefore, we measured ZIKV RNA in the blood at 6 dpi, and in the brain, ovaries, and testis tissues collected from mice at 14 dpi.

At 6 dpi, viral RNA levels in the blood (Figure 3-A) were significantly higher in male mice than in females across all diet groups ($p \leq 0.0001$). However, within each sex, no significant differences in blood viral titers were observed between the different diet groups. In reproductive tissues (Figure 3-B), viral genome copies were consistently higher in the testes compared to the ovaries, regardless of dietary group. No significant differences in viral loads were found among the diet groups for either sex. A distinct pattern emerged in brain tissues (Figure 3-C). ZIKV RNA levels in the brains of mice on the selenium and vitamin E double-deficient diet (SED) were substantially higher than those in mice on the normal (ND) or selenium-deficient (SD) diets. This increase was observed in both male and female mice but was statistically significant for male mice only ($p \leq 0.0082$). In contrast, viral genome copies in the brains of ND and SD groups were similar between sexes and remained much lower than those seen in the SED group.

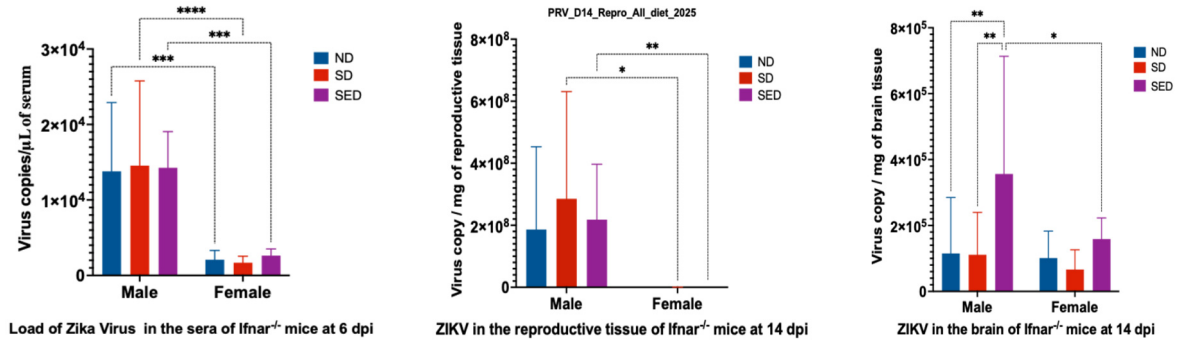

Figure 3. ZIKV RNA genome copies in blood, reproductive, and brain tissues of infected mice. (A) ZIKV genome copies in blood of mice at 6 days post infection. (B) ZIKV genome copies in reproductive tissues (testes and ovaries) of mice at 14 days post infection. (C) ZIKV genome copies in brain tissue of mice at 14 days post infection. ND: Normal diet. SD: Selenium-deficient diet. SED: Selenium and vitamin E double-deficient diet Only significant p values (≤ 0.05), indicated with asterisks, are shown on the figure.

3.4. Genome Diversity and Mutation Analysis Across Dietary Groups

To assess the impact of dietary selenium and vitamin E deficiency on ZIKV genome diversity and mutation accumulation, we analyzed viral sequences from serum, reproductive tissues, and brain samples of male and female mice maintained on the three dietary regimens. Genome diversity was quantified using GINI entropy (Figure 4). No statistically significant differences in overall genome diversity were detected between the three diet groups. However, subtle tissue- and sex-specific variations were observed. In serum samples, the SED group showed a marginally higher genome diversity, while the lowest diversity was observed in the SD group. Analysis of reproductive tissues revealed that ovarian samples consistently exhibited slightly higher diversity than testicular samples across all dietary groups.

 doi:10.20944/preprints202512.1390.v1

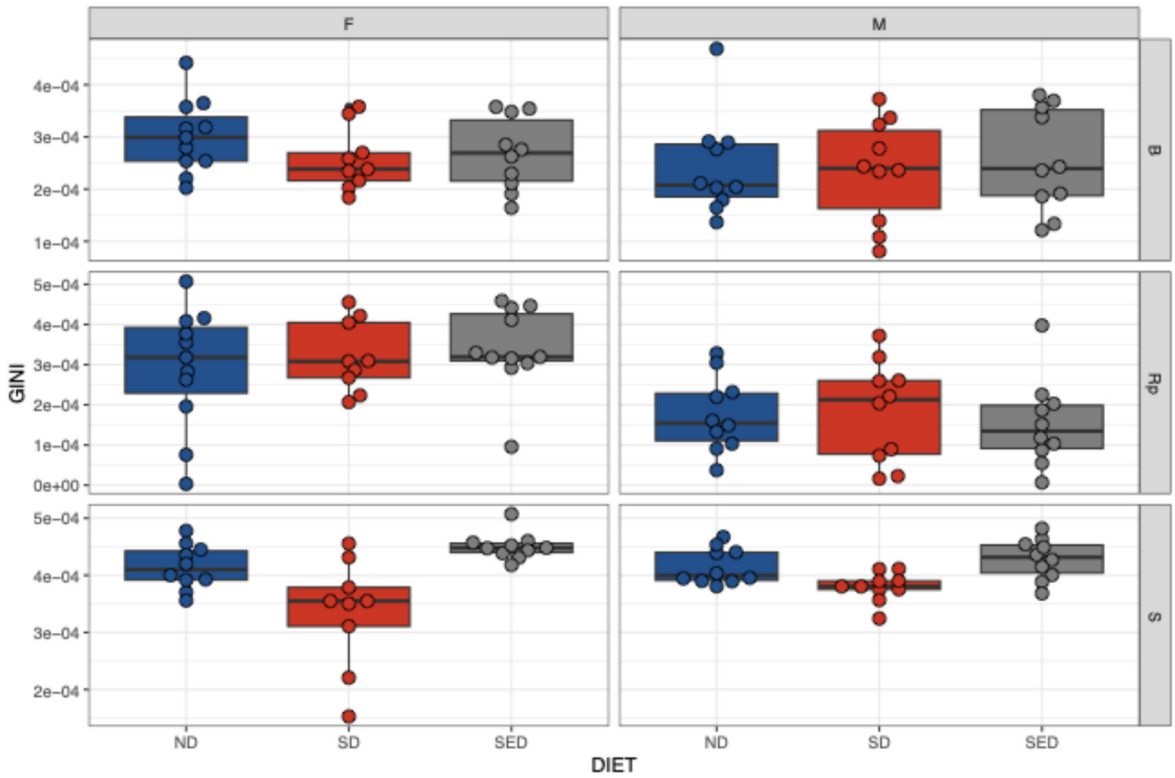

Figure 4. Tissue- and Sex-Specific Genome Diversity of ZIKV Across Dietary Groups. GINI entropy plots depict viral genome diversity in brain, reproductive tissue, and serum samples from female and male mice fed with normal diet (ND), selenium-deficient diet (SD), or selenium plus vitamin E double-deficient diet (SED). Each subplot represents a distinct tissue and sex combination, with GINI entropy values on the y-axis and diet groups on the x-axis. The data illustrate subtle differences in viral diversity across tissues, sexes, and dietary conditions.

3.5. Mutation Landscape

Detailed analysis of the viral genomes revealed several mutations, some of which differed from previously reported variants. Notably, the V330L mutation in the E gene was enriched from an allele frequency of 63.51% in the stock virus used for mouse infection to 86.5% and 93.22% in the reproductive tissues and brain of SED-fed mice, respectively. Another notable mutation, D67E in the E gene, was detected in the brain of SED-fed mice. Additionally, the V360I mutation in the NS3 gene was identified in brain and serum samples from both male and female mice within the SED-fed group. A summary of all detected mutations is provided in Table 2.

Table 2. Notable Mutations Detected in ZIKV Genomes from Mice on Different Diets.

Diet	No.	Sex	Tissue	AF (%)	Gene	AA Pos.	Observed Mut	Reported Mut	Reference
SED	1	F	Rp	4.91	C	106	A106T	T106A	Yu et al.[65]
SD	1	F	S	1.20	C	106	A106V	T106A	
SED	1	F	Rp	13.39	Pr	17	N17S	S17N	Yuan et al.[66]
ND	1	F	Rp	1.71	Pr	17	N17S	S17N	
SED	1	M	B	27.65	E	317	I317L	I317V	Aziz et al.[67]
SD	1	F	Rp	2.43	E	317	I317T	I317V	
SED	1	M	B	93.22	E	330	V330L	V330L	Carbaugh et al[68]
SED	4	M	Rp	69.2–86.5	E	330	V330L		

 doi:10.20944/preprints202512.1390.v1

SD	1	M	Rp	64.82	E	330	V330L		
Input V	1			63.51	E	330	V330L		
SED	1	F	B	1.04	E	367	D67E	D67N	Liu et al.[69]
SD	1	M	S	1.23	E	487	M487V	T487M	Aziz et al.[67]
SED	1	M	B	3.50	NS1	188	V188A	V188A	Liu et al.[69]
SD	1	M	B	2.53	NS1	349	M349T	M349V	Collette et al.[70]
SED	1	M	B	6.82	NS3	360	V360I	V360I	Aziz et al.[67]
SED	1	F	S	1.18	NS3	360	V360I	V360I	
SD	1	F	S	1.07	NS3	584	H584Q	H584Y	Collette et al.[70]

Abbreviations: ND, normal diet; SD, selenium-deficient diet; SED, selenium plus vitamin E double-deficient diet; Input V, input virus; F, female; M, male; S, serum; Rp, reproductive tissue; B, brain; AF, allele frequency.

3.6. Production of Neutralizing Antibody

Selenium and vitamin E are key antioxidants that play a critical role in regulating immune responses, including the production of neutralizing antibodies. Previous studies have demonstrated that deficiencies in these micronutrients impair antibody production and weaken antiviral defenses [5,71,72]. We hypothesized that selenium deficiency, alone or in combination with vitamin E deficiency, would result in reduced neutralizing antibody production in ZIKV-infected mice. Mice maintained on the normal diet exhibited significantly higher neutralizing antibody titers compared to both nutritionally deficient groups. The selenium-deficient and selenium plus vitamin E double-deficient groups showed comparable $PRNT_{50}$ titers, both of which were significantly lower than those observed in the normal diet group (Figure 4). Statistical analysis confirmed that $PRNT_{50}$ titers in the ND group were significantly higher than those in the SD ($p = 0.0245$) and SED groups ($p = 0.0254$).

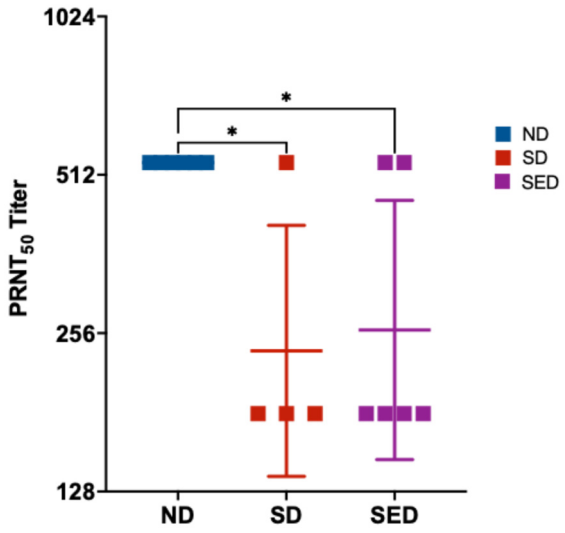

Figure 5. Neutralizing antibody titers ($PRNT_{50}$) in mice from different dietary groups following ZIKV infection. Serum samples were collected 14 days post-infection from mice maintained on a normal diet, selenium-deficient diet, or selenium plus vitamin E double-deficient diet. Neutralizing antibody titers were determined by plaque reduction neutralization test (PRNT). Data are presented as individual values with group means ± SD. *$p < 0.05$ compared to normal diet group.

 doi:10.20944/preprints202512.1390.v1

3.7. Cytokine Responses to ZIKV Infection

Cytokine activation is crucial for combatting ZIKV infection, and poor nutritional status can negatively impact expression of antiviral cytokines [73]. Results from the LEGENDPlex panel revealed distinct patters of immune modulation across the dietary groups. In SD and SED mice IFN-α, IFN-ɣ, and TNF-α expression were all significantly reduced compared to ND mice (Figure 6, A - C). IFN-β expression was significantly reduced in SD mice but was not significantly changed in the SED mice relative to ND mice (Figure 6 D). SD mice showed decreased expression of CCL5 compared to ND (Figure 6 E), while SED mice showed decreased expression of IL-12 (Figure 6 F) and increased expression of GM-CSF (Figure 6 G). Interestingly, several cytokines showed differential expression changes between the deficient diet groups while remaining comparable to expression in ND mice. IFN-β and CCL5 expression were significantly reduced in SD mice but not significantly different between ND and SED mice. Expression was unchanged between ND and SED mice but significantly lower in SD mice. GM-CSF expression was significantly higher in SED mice compared to ND and SD mice, with levels unchanged between ND and SD mice. IL-12(p70) showed a unique trend, where ND and SD expression was not significantly different, SD and SED expression was not significantly different, but SED showed significantly decreased IL-12(p70) expression compared to ND. Other cytokines in the panel showed no significant changes between diet groups (Supplementary Figure S3).

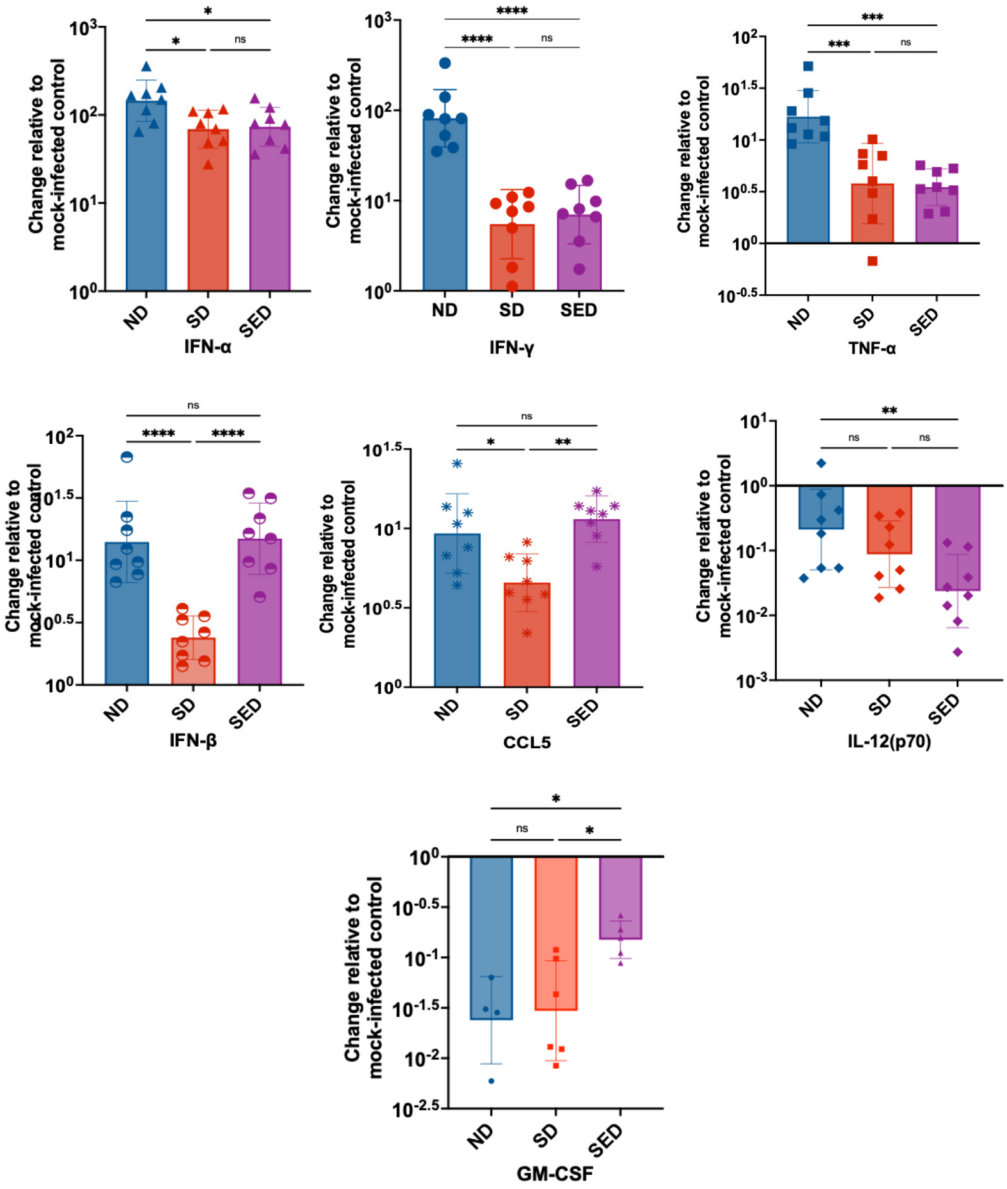

 doi:10.20944/preprints202512.1390.v1

Figure 6. Dietary selenium and vitamin E deficiency modulates antiviral cytokine expression following ZIKV infection. (A–G) Bar plots of cytokines with significant differences between diet groups: (A) IFN-α (B) IFN-γ (C) TNF-α (D) IFN-β (E) CCL5 (F) IL-12p70 (G) GM-CSF. ND: Normal diet; SD: Selenium-deficient diet; SED: Selenium and vitamin E double-deficient diet.

4. Discussion

This study demonstrates that combined dietary deficiency of selenium and vitamin E significantly exacerbates ZIKV neuroinvasion and disease severity in Ifnar-/- mice, while having minimal impact on systemic viral spread and overall viral genome diversity. These findings highlight the critical role of antioxidant micronutrients in modulating host susceptibility to neurotropic viral infections [74,75] and reveal important tissue- and sex-specific patterns in ZIKV pathogenesis.

4.1. Micronutrient Deficiency Increases ZIKV Neurotropism and Disease Severity

Mice maintained on a selenium and vitamin E double-deficient diet (SED) exhibited markedly higher ZIKV RNA levels in the brain, greater weight loss, and increased mortality compared to those on normal or selenium-deficient diets. This supports the hypothesis that antioxidant micronutrients act synergistically to protect against viral neuroinvasion and neuropathology, similar to reports in other studies [5,7,10,76,77]. The impact of combined deficiency, as opposed to single micronutrient deficiency, is consistent with previous reports that the compensatory antioxidant effect of one micronutrient is lost when both are absent [1,26]. The selective increase in brain viral load, rather than systemic dissemination, suggests that both selenium and vitamin E are particularly important for maintaining central nervous system (CNS) antiviral defenses, potentially through mitigation of local oxidative stress [78–80].

4.2. Impaired Immune Responses in Deficient Mice

Both the SD and SED groups exhibited significantly reduced neutralizing antibody titers, indicating a compromised adaptive immune response. Vitamin E is one of the most abundant micronutrients in immune cells, where it protects polyunsaturated fatty acids in cell membranes from oxidative damage [71]. Deficiency in vitamin E has been shown to impair humoral and adaptive immune responses, resulting in diminished antibody production and weakened immune defenses [71,72]. Similarly, selenium deficiency has been associated with reduced antibody responses to viral infections, primarily through impaired B cell function and decreased antibody synthesis [5,77].

In addition to reduced antibody titers, mice in both SD and SED groups showed significantly decreased serum levels of key cytokines, including IFN-α, IFN-γ, and TNF-α. Type I interferons, such as IFN-α, are crucial for initiating antiviral innate immune responses [81–83]. IFN-γ is produced by antigen-presenting cells and adaptive immune cells in response to infection and plays a major role in activating antiviral CD4+ T helper cells [84]. TNF-α is involved in promoting inflammation, inducing apoptosis of infected cells, and facilitating leukocyte adhesion and migration across the endothelium [83]. The expression of these cytokines is typically upregulated during ZIKV infection, and our data demonstrated that SD and SED diet conditions significantly suppressed their expression. This decrease in major regulatory cytokines can have wide-ranging consequences, including increased tissue damage, impaired immune cell recruitment, and diminished activation of antiviral responses. Notably, the marked reduction in IFN-γ expression is consistent with previous findings that selenium deficiency leads to decreased T cell proliferation and lower serum immunoglobulin levels [85], supporting our observation of reduced ZIKV-neutralizing antibodies in these groups.

For the remaining cytokines in the panel (IL-1β, IL-6, IL-10, IL-12(p70), CCL2, CCL5, CXCL1, CXCL10, and GM-CSF), several were differentially expressed between normal diet and deficient diet groups but generally were not impacted by diet or upstream changes in IFN-γ and TNF-α expression. This is curious given that several of these cytokines are regulated by IFN-γ, and TNF-α, such as CCL2, CCL5, IL-1β, IL-6, IL-10, and IL-12(p70) [83]. Our data suggest that expression of interleukins and

 doi:10.20944/preprints202512.1390.v1

other chemokines may not be directly impacted by diet background, and if their regulatory cytokines are differentially expressed, alternative mechanisms may allow for their typical expression.

It is important to note that the mouse model used in this study lacks the type I interferon α/β receptor, which prevents the downstream signaling cascade necessary for effective antiviral protection. However, this genetic modification does not affect the expression of IFN-α and IFN-β themselves, as the genes encoding these cytokines remain intact. Therefore, the cytokine expression data presented here remain valid and informative, despite the absence of receptor-mediated signaling [86].

4.3. Viral Genome Diversity and Mutation Patterns

Previous studies have demonstrated that deficiencies in antioxidant micronutrients, such as selenium, can drive the evolution of increased viral diversity and virulence in several RNA viruses, including influenza virus, coxsackievirus, and HIV [44,46,61,87]. However, in the present study, we did not observe significant differences in ZIKV genome diversity between mice fed adequate and deficient diets. This contrasting finding suggests that the relationship between antioxidant micronutrient deficiency and viral evolution may not be universal across all viruses. It remains unclear whether selenium and vitamin E deficiencies have no impact on ZIKV evolution in this study, or whether the single infection time point and absence of serial inter-host passages limited the opportunity for the emergence and amplification of the expected viral diversity. Previous research has shown that repeated serial passage can be a critical factor in revealing the effects of host nutritional status on viral evolution [46,61]. Supporting this, data from our laboratory indicate that serially passaged SARS-CoV-2 isolates in selenium-deficient BALB/c mice exhibited markedly increased viral diversity compared to those in mice on a nutritionally adequate diet[88].

Despite the lack of statistically significant differences in overall ZIKV diversity between diet groups, we did observe subtle tissue and sex-specific patterns, with slightly elevated viral diversity in the sera and reproductive tissues of selenium-deficient female mice. This observation is noteworthy, as severe outcomes of ZIKV infection, such as neurological impairment and microcephaly, are linked to vertical transmission during pregnancy [89,90]. Viral populations with greater diversity may be better equipped to establish fetal infection and contribute to the development of severe congenital disease [70,91]. However, further research using pregnant, nutrient-deficient mouse models is needed to clarify the relationship between maternal micronutrient status, ZIKV diversity, and the risk of fetal infection.

4.4. Sex-Specific Differences in Viral Load

Male mice consistently exhibited higher viral load in blood and reproductive tissues including mice fed SD and SED diets. The detection of high ZIKV load in the testes at day 14 post-infection indicates persistent infection and viral residence within male reproductive tissues. This finding is particularly significant for sexual transmission, as it suggests that infected males could facilitate the spread of novel variants via an alternate transmission route. The public health implications are considerable, especially if direct host-to-host transmission, combined with nutritional deficiency, contributes to the emergence of more virulent viral strains, as has been observed with other viruses such as influenza and Coxsackie virus [92].

4.5. Mutation Analysis and Potential Functional Implications

Several notable mutations were identified in the viral genomes from various tissues and dietary groups in our study. Although these mutations did not correlate with distinct or unique phenotypic manifestations in the host within our experiments, the implications of some have been described in the literature. The V330L mutation in the E gene, previously reported as attenuating in Ifnar1−/− mice infected with the PRVABC59 strain of ZIKV [68,93], was present in the stock virus and detected across all experimental groups. Notably, this substitution appeared at higher allele frequencies in brain and

 doi:10.20944/preprints202512.1390.v1

reproductive tissue samples from males in the SED and SD groups, suggesting possible enrichment under deficient conditions. This observation, particularly in male mice, warrants further investigation into its biological significance. Furthermore, the D67E mutation on the E gene was detected in the brain of a female mouse from the SED diet group. Notably, mutation at this position (D67N) has been reported to markedly increase neurovirulence in mice [69], suggesting that substitutions at this site may have important functional implications for viral pathogenesis.

The V360I mutation in the NS3 gene, previously described in other ZIKV isolates [67], was detected in the brain and serum of both male and female mice within the SED group. The implication of this mutation is not known and the fact that it is within the helicase region of the NS3 [94] makes it interesting for future studies.

Although these mutations were observed in a limited number of animals, their presence highlights the potential for rare variants to emerge and persist under selective pressures, particularly in the context of nutritional deficiencies. Over time and with repeated host-to-host transmission, such mutations could acquire epidemiological significance.

4.6. Clinical and Public Health Implications

These findings have important implications for populations at risk of micronutrient deficiencies, particularly in regions endemic for ZIKV and other neurotropic pathogens. Ensuring adequate selenium and vitamin E intake may be critical for reducing the risk of severe neurological complications and improving outcomes during viral outbreaks [5,6]. Nutritional interventions could serve as adjuncts to vaccination and antiviral therapies, especially in vulnerable groups [9].

4.7. Limitations and Future Directions

This study provides valuable insights into the effects of antioxidant micronutrient deficiencies on ZIKV infection and viral evolution in mice. However, our experimental model focused on individual animals and did not address viral evolution across multiple hosts within a population. As a result, we were unable to assess how rare mutations might be selected for, maintained, or spread through repeated host-to-host transmission. In addition, three mice deaths were recorded during the study, but samples could not be collected from these animals for processing due to existing animal facility protocols. Therefore, we are unable to determine how information from the mice that died could have impacted the equilibrium of genetic diversity and mutation observed in this research. Future research utilizing population-based or serial passage models will be essential to determine whether such mutations can acquire epidemiological significance over time, as has been observed with serial passage of SARS-CoV-2 in our laboratory [95].While the use of Ifnar-/- mice provides a sensitive model for studying ZIKV pathogenesis, it may not fully recapitulate the immune responses of immunocompetent hosts. Additionally, while we identified several potentially important viral mutations, their functional consequences, particularly regarding viral fitness, pathogenicity, and drug sensitivity, remain largely unexplored. Follow-up studies using reverse genetics and in vivo challenge models will be necessary to clarify the roles of these variants.

Supplementary Materials: The following supporting information can be downloaded at the website of this paper posted on Preprints.org. **Table S1. Composition of experimental diets. Table S2.** Custom-designed sequencing primers (M1000) for multiplex amplification of Zika virus strains PRVABC59 and FSS13025. **Figure S1. Quantification of Zika virus RNA genome copies in blood and brain tissues. Figure S2. Sequencing Coverage Profiles Obtained with the M1000 Primer Set. Figure S3. Dietary selenium and vitamin E deficiency impacts cytokine responses to Zika virus infection.**

Author Contributions: "Conceptualization, MB, NC, OO; methodology, MB, OO, NC, DW; software, AA, JK; validation, OO, MB, JT, JK, AA.; formal analysis, OO, MB, JK, AA, JT; investigation, OO, NC, DM, MG, TT; resources, MB, NC, DW; data curation, JT, JK, AA; writing—original draft preparation, OO, MG; writing—review and editing, OO, MB, MG, NC, DW, AA, JK; visualization, OO, JK; supervision, MB, NC; project

 doi:10.20944/preprints202512.1390.v1

administration, MB; funding acquisition, MB, NC, DW. All authors have read and agreed to the published version of the manuscript.

Funding: This research was funded by the Department of Energy, Lawrence Livermore National Laboratory, Laboratory Directed Research & Development grant number LDRD 23-ERD-012.

Data Availability Statement: The original data presented in the study are openly available in NCBI Sequence Read Archive under BioProject accession number PRJNA1374194.

Acknowledgments: This work was performed under the auspices of the U.S. Department of Energy by Lawrence Livermore National Laboratory under Contract DE-AC52-07NA27344. The following reagent was obtained through BEI Resources: PRVABC59 strain (Human/2015/Puerto Rico) NR-50240.

Conflicts of Interest: The authors declare no conflicts of interest.

References

1. Carlson BA, Tobe R, Yefremova E, Tsuji PA, Hoffmann VJ, Schweizer U, et al. Glutathione peroxidase 4 and vitamin E cooperatively prevent hepatocellular degeneration. Redox Biol. 2016;9:22-31.
2. Combs GF, Jr. Selenium in global food systems. Br J Nutr. 2001;85(5):517-47.
3. Wang M, Li Y, Molenaar A, Li Q, Cao Y, Shen Y, et al. Vitamin E and selenium supplementation synergistically alleviate the injury induced by hydrogen peroxide in bovine granulosa cells. Theriogenology. 2021;170:91-106.
4. Rotruck JT, Pope AL, Ganther HE, Swanson AB, Hafeman DG, WG H. Selenium: biochemical role as a component of glutathione peroxidase. Science. 1973;179(4073):588 - 90.
5. Beck MA, Levander OA, Handy J. Selenium deficiency and viral infection. J Nutr. 2003;133(5 Suppl 1):1463S-7S.
6. Steinbrenner H, Speckmann B, Sies H. Toward Understanding Success and Failures in the Use of Selenium for Cancer Prevention. Antioxidants & Redox Signaling. 2013;19(2):181-91.
7. Beck MA. Selenium and vitamin E status: impact on viral pathogenicity. J Nutr. 2007;137(5):1338-40.
8. Beck MA. Increased virulence of coxsackievirus B3 in mice due to vitamin E or selenium deficiency. J Nutr. 1997;127(5 Suppl):966S-70S.
9. García AH, Crespo FI, Mayora SJ, Martinez WY, Belisario I, Medina C, et al. Role of Micronutrients in the Response to SARS-CoV-2 Infection in Pediatric Patients. Immuno. 2024;4(3):211-25.
10. Martinez SS, Huang Y, Acuna L, Laverde E, Trujillo D, Barbieri MA, et al. Role of Selenium in Viral Infections with a Major Focus on SARS-CoV-2. Int J Mol Sci. 2021;23(1).
11. Mansour U M, Salem H,A. EFFECT OF SELENIUM AND /OR VITAMIN E ON BOVINE HERPES TYPE 1 INFECTION IN VITRO CULTURED CELLS. AVMJ. 2015;61(146):87 - 95.
12. Gowder SJ. Critical Analysis of Selenium Deficiency Diseases: An Overview. American Journal of Biomedical Science and Research. 2024;24(2):151 - 2.
13. Zhang HY, Zhang AR, Lu QB, Zhang XA, Zhang ZJ, Guan XG, et al. Association between fatality rate of COVID-19 and selenium deficiency in China. BMC Infect Dis. 2021;21(1):452.
14. Fang LQ, Goeijenbier M, Zuo SQ, Wang LP, Liang S, Klein SL, et al. The association between hantavirus infection and selenium deficiency in mainland China. Viruses. 2015;7(1):333-51.
15. Ge K, Yang G. The epidemiology of selenium deficiency in the etiological study of endemic diseases in China. Am J Clin Nutr. 1993;57(2 Suppl):259S-63S.
16. Yang C, Yao H, Wu Y, Sun G, Yang W, Li Z, et al. Status and risks of selenium deficiency in a traditional selenium-deficient area in Northeast China. Sci Total Environ. 2021;762:144103.
17. Rayman MP. Selenium and human health. Lancet. 2012;379(9822):1256-68.
18. Maggini S, Wintergerst ES, Beveridge S, Hornig DH. Selected vitamins and trace elements support immune function by strengthening epithelial barriers and cellular and humoral immune responses. Br J Nutr. 2007;98 Suppl 1:S29-35.
19. Li SJ, Wang AW, Huang KL, Yang Y. Recent Advances on Selenium Nutrition and Keshan Disease. Int Heart J. 2024;65(2):173-9.

 doi:10.20944/preprints202512.1390.v1

20. Kryukov GV, Castellano S, Novoselov SV, Lobanov AV, Zehtab O, Guigo R, et al. Characterization of mammalian selenoproteomes. Science. 2003;300(5624):1439-43.
21. Labunskyy VM, Hatfield DL, Gladyshev VN. Selenoproteins: molecular pathways and physiological roles. Physiol Rev. 2014;94(3):739-77.
22. Papp LV, Lu J, Holmgren A, Khanna KK. From selenium to selenoproteins: synthesis, identity, and their role in human health. Antioxid Redox Signal. 2007;9(7):775-806.
23. Traber MG, Atkinson J. Vitamin E, antioxidant and nothing more. Free Radic Biol Med. 2007;43(1):4-15.
24. Cheng WH, Valentine BA, Lei XG. High levels of dietary vitamin E do not replace cellular glutathione peroxidase in protecting mice from acute oxidative stress. J Nutr. 1999;129(11):1951-7.
25. Levander OA. Nutrition and newly emerging viral diseases: an overview. J Nutr. 1997;127(5 Suppl):948S-50S.
26. Wortmann M, Schneider M, Pircher J, Hellfritsch J, Aichler M, Vegi N, et al. Combined deficiency in glutathione peroxidase 4 and vitamin E causes multiorgan thrombus formation and early death in mice. Circ Res. 2013;113(4):408-17.
27. Jones GD, Droz B, Greve P, Gottschalk P, Poffet D, McGrath SP, et al. Selenium deficiency risk predicted to increase under future climate change. Proc Natl Acad Sci U S A. 2017;114(11):2848-53.
28. Winkel LH, Vriens B, Jones GD, Schneider LS, Pilon-Smits E, Banuelos GS. Selenium cycling across soil-plant-atmosphere interfaces: a critical review. Nutrients. 2015;7(6):4199-239.
29. Beck MA, Levander OA. Host nutritional status and its effect on a viral pathogen. J Infect Dis. 2000;182 Suppl 1:S93-6.
30. Holland J, Spindler K, Horodyski F, Grabau E, Nichol S, VandePol S. Rapid evolution of RNA genomes. Science. 1982;215(4540):1577-85.
31. Domingo E, Sheldon J, Perales C. Viral quasispecies evolution. Microbiol Mol Biol Rev. 2012;76(2):159-216.
32. Moya A, Elena SF, Bracho A, Miralles R, Barrio E. The evolution of RNA viruses: A population genetics view. Proc Natl Acad Sci U S A. 2000;97(13):6967-73.
33. Kieliszek M, Bano I, Zare H. A Comprehensive Review on Selenium and Its Effects on Human Health and Distribution in Middle Eastern Countries. Biol Trace Elem Res. 2022;200(3):971-87.
34. Musso D, Gubler DJ. Zika Virus. Clin Microbiol Rev. 2016;29(3):487-524.
35. Petersen LR, Jamieson DJ, Powers AM, Honein MA. Zika Virus. N Engl J Med. 2016;374(16):1552-63.
36. Vignuzzi M, Stone JK, Arnold JJ, Cameron CE, Andino R. Quasispecies diversity determines pathogenesis through cooperative interactions in a viral population. Nature. 2006;439(7074):344-8.
37. van Boheemen S, Tas A, Anvar SY, van Grootveld R, Albulescu IC, Bauer MP, et al. Quasispecies composition and evolution of a typical Zika virus clinical isolate from Suriname. Sci Rep. 2017;7(1):2368.
38. Coffey LL, Beeharry Y, Borderia AV, Blanc H, Vignuzzi M. Arbovirus high fidelity variant loses fitness in mosquitoes and mice. Proc Natl Acad Sci U S A. 2011;108(38):16038-43.
39. Grubaugh ND, Weger-Lucarelli J, Murrieta RA, Fauver JR, Garcia-Luna SM, Prasad AN, et al. Genetic Drift during Systemic Arbovirus Infection of Mosquito Vectors Leads to Decreased Relative Fitness during Host Switching. Cell Host Microbe. 2016;19(4):481-92.
40. Brasil P, Pereira JP, Jr., Moreira ME, Ribeiro Nogueira RM, Damasceno L, Wakimoto M, et al. Zika Virus Infection in Pregnant Women in Rio de Janeiro. N Engl J Med. 2016;375(24):2321-34.
41. Cao-Lormeau VM, Blake A, Mons S, Lastere S, Roche C, Vanhomwegen J, et al. Guillain-Barre Syndrome outbreak associated with Zika virus infection in French Polynesia: a case-control study. Lancet. 2016;387(10027):1531-9.
42. Yakob L. Zika Virus after the Public Health Emergency of International Concern Period, Brazil. Emerg Infect Dis. 2022;28(4):837-40.
43. Musso D, Ko AI, Baud D. Zika Virus Infection - After the Pandemic. N Engl J Med. 2019;381(15):1444-57.
44. Baum MK, Shor-Posner G. Micronutrient status in relationship to mortality in HIV-1 disease. Nutr Rev. 1998;56(1 Pt 2):S135-9.
45. Oluwasemowo OO, Graham ME, Murugesh DK, Borucki MK. Improved Zika virus plaque assay using Vero/TMPRSS2 cell line. Microbiol Spectr. 2025;13(1):e0162424.

 doi:10.20944/preprints202512.1390.v1

46. Heather K. Nelson QS, Peter Van Dael, Eduardo J. Schiffrin, Stephanie Blum, Denis Barclay, Orville A. Levander, and Melinda A. Beck. Host nutritional selenium status as a driving force for Influenza virus mutations. FASEB J. 2001;15(10):1727 - 38.
47. Sunde RA. Selenium. In: A. C. Ross BC, R. J. Cousins, K. L. Tucker and T. R. Ziegler, editor. Modern Nutrition in Health and Disease. 11th ed: Wolters Kluwer; 2016. p. 225 –37.
48. EFSA NDA Panel (EFSA Panel on Dietetic Products NaA. Scientific Opinion on Dietary Reference Values for selenium. EFSA Journal. 2014;12(10).
49. Winkler CW, Peterson KE. Using immunocompromised mice to identify mechanisms of Zika virus transmission and pathogenesis. Immunology. 2018;153(4):443-54.
50. Johnson KEE, Noval MG, Rangel MV, De Jesus E, Geber A, Schuster S, et al. Mapping the evolutionary landscape of Zika virus infection in immunocompromised mice. Virus Evol. 2020;6(2):veaa092.
51. Smith AD, Botero S, Shea-Donohue T, Urban JF, Jr. The pathogenicity of an enteric Citrobacter rodentium Infection is enhanced by deficiencies in the antioxidants selenium and vitamin E. Infect Immun. 2011;79(4):1471-8.
52. Lanciotti RS, Kosoy OL, Laven JJ, Velez JO, Lambert AJ, Johnson AJ, et al. Genetic and serologic properties of Zika virus associated with an epidemic, Yap State, Micronesia, 2007. Emerg Infect Dis. 2008;14(8):1232-9.
53. Dia M, Bob NS, Talla C, Dupressoir A, Escadafal C, Thiam MS, et al. Performance assessment and validation of a plaque reduction neutralization test (PRNT) in support to yellow fever diagnostic and vaccine clinical trials. J Med Virol. 2023;95(4):e28700.
54. Quick J, Grubaugh ND, Pullan ST, Claro IM, Smith AD, Gangavarapu K, et al. Multiplex PCR method for MinION and Illumina sequencing of Zika and other virus genomes directly from clinical samples. Nat Protoc. 2017;12(6):1261-76.
55. Grubaugh ND, Gangavarapu K, Quick J, Matteson NL, De Jesus JG, Main BJ, et al. An amplicon-based sequencing framework for accurately measuring intrahost virus diversity using PrimalSeq and iVar. Genome Biol. 2019;20(1):8.
56. Kimbrel J, Moon J, Avila-Herrera A, Marti JM, Thissen J, Mulakken N, et al. Multiple Mutations Associated with Emergent Variants Can Be Detected as Low-Frequency Mutations in Early SARS-CoV-2 Pandemic Clinical Samples. Viruses. 2022;14(12).
57. Team RC. R: A language and environment for statistical computing. 4.5.0 ed. R Foundation for Statistical Computing, Vienna, Austria.2023.
58. Arthur JR. The glutathione peroxidases. CMLS, Cell Mol Life Sci 2001;57:1825 - 35.
59. Lazear HM, Govero J, Smith AM, Platt DJ, Fernandez E, Miner JJ, et al. A Mouse Model of Zika Virus Pathogenesis. Cell Host Microbe. 2016;19(5):720-30.
60. Aliota MT, Caine EA, Walker EC, Larkin KE, Camacho E, Osorio JE. Characterization of Lethal Zika Virus Infection in AG129 Mice. PLoS Negl Trop Dis. 2016;10(4):e0004682.
61. Beck MA, Shi Q, Morris VC, Levander OA. Rapid genomic evolution of a non-virulent coxsackievirus B3 in selenium-deficient mice results in selection of identical virulent isolates. Nat Med. 1995;1(5):433-6.
62. Ball EE, Pesavento PA, Van Rompay KKA, Keel MK, Singapuri A, Gomez-Vazquez JP, et al. Zika virus persistence in the male macaque reproductive tract. PLoS Negl Trop Dis. 2022;16(7):e0010566.
63. Bhatnagar J, Rabeneck DB, Martines RB, Reagan-Steiner S, Ermias Y, Estetter LB, et al. Zika Virus RNA Replication and Persistence in Brain and Placental Tissue. Emerg Infect Dis. 2017;23(3):405-14.
64. Duggal NK, Ritter JM, Pestorius SE, Zaki SR, Davis BS, Chang GJ, et al. Frequent Zika Virus Sexual Transmission and Prolonged Viral RNA Shedding in an Immunodeficient Mouse Model. Cell Rep. 2017;18(7):1751-60.
65. Yu X, Shan C, Zhu Y, Ma E, Wang J, Wang P, et al. A mutation-mediated evolutionary adaptation of Zika virus in mosquito and mammalian host. Proc Natl Acad Sci U S A. 2021;118(42).
66. Yuan L, Huang XY, Liu ZY, Zhang F, Zhu XL, Yu JY, et al. A single mutation in the prM protein of Zika virus contributes to fetal microcephaly. Science. 2017;358(6365):933-6.

 doi:10.20944/preprints202512.1390.v1

67. Aziz A, Suleman M, Shah A, Ullah A, Rashid F, Khan S, et al. Comparative mutational analysis of the Zika virus genome from different geographical locations and its effect on the efficacy of Zika virus-specific neutralizing antibodies. Front Microbiol. 2023;14:1098323.
68. Carbaugh DL, Zhou S, Sanders W, Moorman NJ, Swanstrom R, Lazear HM. Two Genetic Differences between Closely Related Zika Virus Strains Determine Pathogenic Outcome in Mice. J Virol. 2020;94(20).
69. Liu Z, Zhang Y, Cheng M, Ge N, Shu J, Xu Z, et al. A single nonsynonymous mutation on ZIKV E protein-coding sequences leads to markedly increased neurovirulence in vivo. Virol Sin. 2022;37(1):115-26.
70. Collette NM, Lao VHI, Weilhammer DR, Zingg B, Cohen SD, Hwang M, et al. Single Amino Acid Mutations Affect Zika Virus Replication In Vitro and Virulence In Vivo. Viruses. 2020;12(11).
71. Lewis ED, Meydani SN, Wu D. Regulatory role of vitamin E in the immune system and inflammation. IUBMB Life. 2019;71(4):487-94.
72. Lee GY, Han SN. The Role of Vitamin E in Immunity. Nutrients. 2018;10(11).
73. Ngono AE, Shresta S. Immune Response to Dengue and Zika. Annu Rev Immunol. 2018;36:279-308.
74. Doaei S, Mardi A, Zare M. Role of micronutrients in the modulation of immune system and platelet activating factor in patients with COVID-19; a narrative review. Front Nutr. 2023;10:1207237.
75. Pecora F, Persico F, Argentiero A, Neglia C, Esposito S. The Role of Micronutrients in Support of the Immune Response against Viral Infections. Nutrients. 2020;12(10).
76. Sheridan PA, Beck MA. The immune response to herpes simplex virus encephalitis in mice is modulated by dietary vitamin E. J Nutr. 2008;138(1):130-7.
77. Huang Z, Rose AH, Hoffmann PR. The role of selenium in inflammation and immunity: from molecular mechanisms to therapeutic opportunities. Antioxid Redox Signal. 2012;16(7):705-43.
78. Wongchitrat P, Chanmee T, Govitrapong P. Molecular Mechanisms Associated with Neurodegeneration of Neurotropic Viral Infection. Mol Neurobiol. 2024;61(5):2881-903.
79. Ledur PF, Karmirian K, Pedrosa C, Souza LRQ, Assis-de-Lemos G, Martins TM, et al. Zika virus infection leads to mitochondrial failure, oxidative stress and DNA damage in human iPSC-derived astrocytes. Sci Rep. 2020;10(1):1218.
80. Almeida LT, Ferraz AC, da Silva Caetano CC, da Silva Menegatto MB, Dos Santos Pereira Andrade AC, Lima RLS, et al. Zika virus induces oxidative stress and decreases antioxidant enzyme activities in vitro and in vivo. Virus Res. 2020;286:198084.
81. Lazear HM, Schoggins JW, Diamond MS. Shared and Distinct Functions of Type I and Type III Interferons. Immunity. 2019;50(4):907-23.
82. Schoggins JW. Interferon-Stimulated Genes: What Do They All Do? Annu Rev Virol. 2019;6(1):567-84.
83. Bradley JR. TNF-mediated inflammatory disease. J Pathol. 2008;214(2):149-60.
84. Schroder K, Hertzog PJ, Ravasi T, Hume DA. Interferon-gamma: an overview of signals, mechanisms and functions. J Leukoc Biol. 2004;75(2):163-89.
85. Shrimali RK, Irons RD, Carlson BA, Sano Y, Gladyshev VN, Park JM, et al. Selenoproteins mediate T cell immunity through an antioxidant mechanism. J Biol Chem. 2008;283(29):20181-5.
86. Müller U, Steinhoff, U., Reis, L. F. L., Hemmi, S., Pavlovic, J., Zinkernagel, R. M., & Aguet, M. . Functional role of type I and type II interferons in antiviral defense. . Science. 1994;264(5167):1918 - 21.
87. Hiffler L, Rakotoambinina B. Selenium and RNA Virus Interactions: Potential Implications for SARS-CoV-2 Infection (COVID-19). Front Nutr. 2020;7:164.
88. Graham ME; Oluwasemowo OO; Murugesh DK; Avila-Herrera, A; Kimbrel, JA; Phillips, AM; Collette, NM; Weilhammer, DR; Borucki, MK., editor Impacts of Climate-drive Host Selenium Status on SARS-CoV-2 Pathogenesis and Variant Emergence. 44th Annual Meeting, American Society for Virology; 2025 July 14 - 17, 2025; McGill University, Montreal, Quebec, Canada.
89. Rasmussen SA, Jamieson, D. J., Honein, M. A., & Petersen, L. R. . Zika Virus and Birth Defects — Reviewing the Evidence for Causality. New England Journal of Medicine. 2016;374(20):1981 - 7.
90. Mlakar J, Korva M, Tul N, Popovic M, Poljsak-Prijatelj M, Mraz J, et al. Zika Virus Associated with Microcephaly. N Engl J Med. 2016;374(10):951-8.
91. Lemos D SJ, Louie W, Singapuri A, Ramírez AL, Watanabe J, Usachenko J, Keesler RI, Sanchez-San Martin C, Li T, Martyn C, Oliveira G, Saraf S, Grubaugh ND, Andersen KG, Thissen J, Allen J, Borucki M,

 doi:10.20944/preprints202512.1390.v1

Tsetsarkin KA, Pletnev AG, Chiu CY, Van Rompay KKA, Coffey LL. . Two Sides of a Coin: a Zika Virus Mutation Selected in Pregnant Rhesus Macaques Promotes Fetal Infection in Mice but at a Cost of Reduced Fitness in Nonpregnant Macaques and Diminished Transmissibility by Vectors. J Virol. 2020;94(24):e01605-20.

92. Beck MA, Handy J, Levander OA. Host nutritional status: the neglected virulence factor. Trends Microbiol. 2004;12(9):417-23.
93. Duggal NK, McDonald EM, Weger-Lucarelli J, Hawks SA, Ritter JM, Romo H, et al. Mutations present in a low-passage Zika virus isolate result in attenuated pathogenesis in mice. Virology. 2019;530:19-26.
94. Tian H, Ji X, Yang X, Xie W, Yang K, Chen C, et al. The crystal structure of Zika virus helicase: basis for antiviral drug design. Protein Cell. 2016;7(6):450-4.
95. Graham MO, OO; Murugesh, DK; Kimbrel, JA; Avila-Herrera, A; Thissen, J; Zemla, A; Phillips, A; Collette, NM; Weilhammer, DR; Borucki, MK. . Impacts of Host Selenium Status on SARS-CoV-2 Variant Emergence and Pathogenesis. [Manuscript in preparation.]. In press 2025.